A multipass Ti:sapphire laser amplifier pumped with homogenized Nd:YAG lasers

Yi Zheng (郑轶)[1], Jinglong Ma (马景龙)[1*], Xulei Ge (葛绪雷)[1,2], Yutong Li (李玉同)[1], Zhiyi Wei (魏志义)[1], and Jie Zhang (张杰)[1,3]

[1]*Beijing National Laboratory for Condensed Matter Physics, Institute of Physics, Chinese Academy of Sciences, Beijing 100190, China*

[2]*State Key Laboratory of Surface Physics, Department of Physics, Fudan University, Shanghai 200433, China*

[3]*Key Laboratory for Laser Plasmas (MoE), Department of Physics, Shanghai Jiao Tong University, Shanghai 200240, China*

**Corresponding author: majinglong@iphy.ac.cn*

Received March 26, 2014; accepted May 4, 2014; posted online October 20, 2014

A speckle pattern is observed when a neodymium-doped yttrium aluminum garnet (Nd:YAG) laser is homogenized by a diffractive optical element (DOE) due to its high spatial coherence. Therefore, a Nd:YAG laser homogenized by a DOE was previously considered not suitable to pump a Ti:sapphire laser amplifier. However, we show by experiment and simulation that the speckle structure does not manifest itself in the final amplified Ti:sapphire laser beam. By using the homogenizer, a smooth distribution of the amplified laser beam is obtained. No degradation of the energy, the wavefront, and the temporal characteristics of the amplified laser beam is observed.

OCIS codes: 140.3280, 140.3300.

DOI: 10.3788/COL201412.S21412.

Q-switched neodymium-doped yttrium aluminum garnet (Nd:YAG) and Nd:glass lasers are primary pump lasers for high-power femtosecond Ti:sapphire laser systems[1–3]. Nonuniformity in these pump lasers is one of the great concerns that lead to damage of optical components and low extraction efficiency. Therefore, a flat-top pump-beam profile on the crystal is favorable. The relay image technique has been the widely used method to improve the beam quality, but its result strongly depends on the near-field distribution of the pump laser, because it only images the beam profile at the output port to the crystal. Recently, diffractive optical elements (DOEs) are successfully applied to homogenize Nd:glass lasers[2–6]. In this scheme, a pump laser beam is split into multiple beamlets with different phases after passing through a DOE, and the beamlets are superimposed by a lens on the focal plane, forming a homogeneous distribution. The reshaped beam pattern is not sensitive to the input beam distribution, and the effective transmission efficiency can be considerably high[7]. Implementation of a DOE in the existing pumping beam is also quite simple[8]. These features make the DOE very attractive.

However, on applying this technique to a Nd:YAG laser, its high spatial coherence makes it very difficult to cancel out the interference between different beamlets generated by a DOE[9]. The homogenized beam pattern exhibits randomly distributed speckles. The average size of each speckle is roughly that of the pump beam diffraction limit $f\lambda/D$, where f is the focal length of the lens, λ the pump laser wavelength, and D the input beam diameter. For example, the speckle size on the focal plane of a 1200-mm lens for a 532-nm laser beam of diameter 10 mm passing through a DOE is about 62-μm. The image contrast C is close to 100%, which is a measure of the spatial coherence of the laser. The contrast C is defined as $C^2 = (\langle I^2\rangle - \langle I\rangle^2)/\langle I\rangle^2$, where $\langle I\rangle$ is the averaged intensity. For this reason, DOEs are generally considered not applicable to homogenize Nd:YAG lasers as the pump of Ti:sapphire lasers[9–11].

In this paper, we show by experiment and simulation that the speckle pattern does not manifest itself in the final amplified laser beam. In a multipass Ti:sapphire amplifier pumped with such a speckle pattern, the homogeneity and the energy extraction efficiency of the amplified laser beam are improved. The wavefront, focusability, and temporal characteristics of the laser beam are comparable to those with direct pumping.

The experiment is carried out on the last stage amplifier of a multi-terawatt Ti:sapphire laser system Extreme Light II at the Institute of Physics, Chinese Academy of Sciences. In the original setup, two 1-J Nd:YAG laser beams are relay imaged to the Ti:sapphire crystal through two vacuum tubes. The seed pulse is chirped to 240 ps, 6 mJ of energy, 9-mm in diameter, and with a Gaussian spatial distribution. The four-pass amplified laser energy is about 450 mJ, and the compressed pulse width is around 60 fs. From time to time, pump beam profiles vary due to reasons such as misalignment of the cavity and the SHG crystal, damage of the YAG crystal, and degradation of the output coupler coating. Figure 1(a) shows an abnormal pump distribution. In most occasions, such a distribution led to damage of mirrors in the amplifier and the last grating in the compressor. For this reason, laser amplification is far below saturation.

To improve the spatial quality of the amplified beam, the relay imaging vacuum tubes are replaced by two identical DOEs (SILIOS Technologies), which were designed to form a round shape on the focal plane of a 1200-mm lens, as shown in Fig. 2. We obtain about 80% of the input energy in the central spot on the crystal.

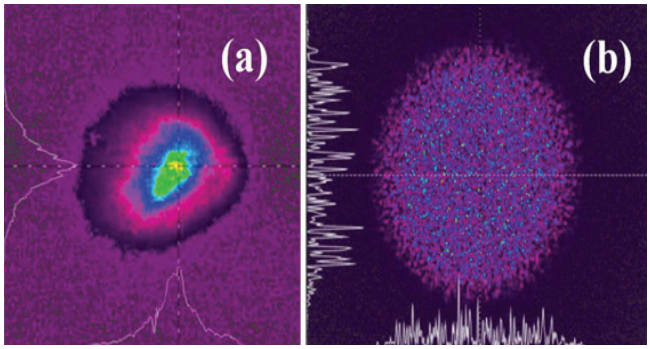

Fig. 1. (a) Direct pump beam and (b) DOE homogenized pump beam, not in same scale as in panel a.

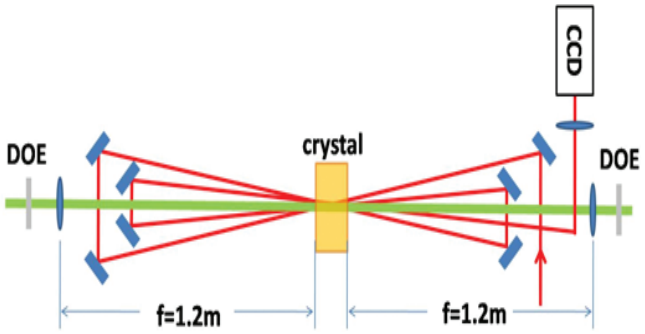

Fig. 2. Setup of the DOEs in the amplifier.

The zero-order diffraction is out of the crystal and blocked by the crystal mount.

Figure 1(b) shows one homogenized beam pattern at the focal plane of the lens, which is composed of multiple tiny speckles, with average diameter around 60-μm. The speckles account for around 70% of the spot area. The image contrast is close to unit. This shows that the Nd:YAG laser is highly coherent. Fine fluorescent striations can be observed through the Ti:sapphire crystal when it is illuminated with the DOE homogenized pump laser. The highest energy density in the brightest speckle to the average across the image is measured to be seven times. In the experiment, the averaged energy density is 1.3 J/cm^2, so the highest energy density is about 9 J/cm^2. However, no damage on the crystal induced by these tiny speckles is observed.

With a total pump energy of 1.6 J in two directions, the amplified laser energy is 450 mJ, comparable to that with 2-J direct pumping. The higher extraction efficiency can be attributed to the higher gain for the weaker part in the input beam. Figure 3 shows the distributions of the amplified laser beams with direct pumping and a DOE homogenized pumping, the difference is quite extinct. The directly pumped laser beam shows intense peaks in the center obviously related with the pump beam profile, as shown in Fig. 3(a). In the latter case, dotted structure is observed in the amplified beam pattern after its first pass through the crystal, but not in the following passes. Finally, a uniform beam is obtained as shown in Fig. 3(b). Please note defects in the neutral density filter contribute some nonuniformity in the measured beam

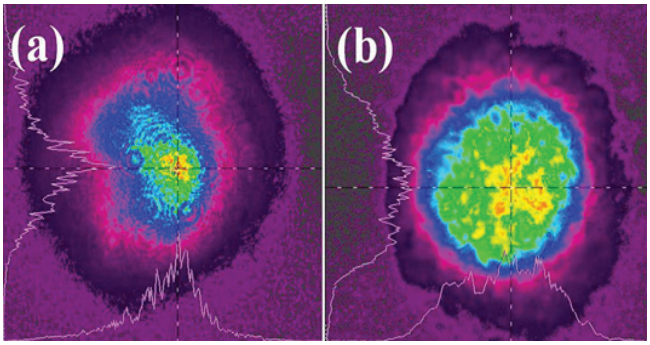

Fig. 3. Amplified laser beam with (a) direct pump and (b) DOE homogenized pump.

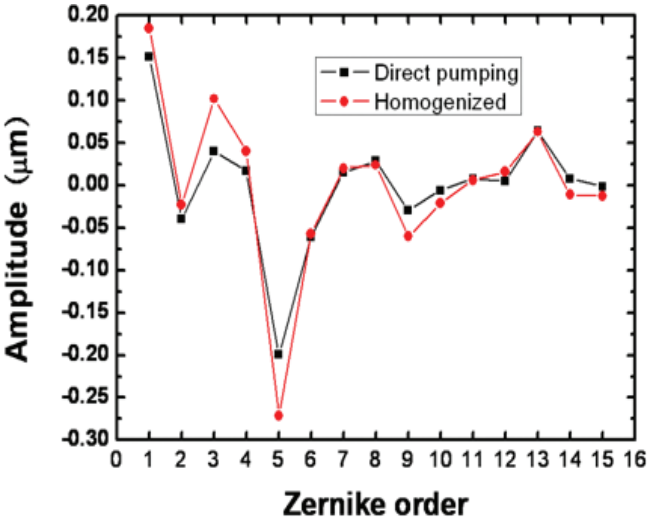

Fig. 4. Zernike coefficients of the amplified laser beam. (1) Piston, (2) Tip y, (3) Tilt x, (4) Astigmatism ±45°, (5) Defocus, (6) Astigmatism 0/90°, (7) Trefoil y, (8) Coma x, (9) Coma y, (10) Trefoil x, (11) Tetrafoil x, (12) Secondary Astigmatism y, (13) Spherical, (14) Secondary Astigmatism x, (15) Tetrafoil x.

pattern. Laser operation in hundreds of hours shows no damage occurred on mirrors and the compression gratings. This is a significant improvement compared with previous operation with direct pumping.

Wavefronts of the amplified laser beams are measured with a Shack–Hartmann sensor (WFS150-7AR; Thorlabs). The comparison of the direct pumping and the DOE homogenized pumping is shown in Fig. 4. The piston, tip, tilt, and defocus are dependent on measurement geometry and are trivial for characterizing a real laser beam. The rest Zernike coefficients of the two cases are very close. Another measurement is also taken to compare the focused spot size. With a same focal monitor in the target chamber, the expanded and compressed laser beam is focused by an off-axis parabolic mirror. The two foci are shown in Fig. 5. They appear very similar and are about 1.3 times of the diffraction limit.

Temporal characteristics of the laser pulse after compression are characterized with a single-shot autocorrelator (Delta AC; Minioptic Technology) and

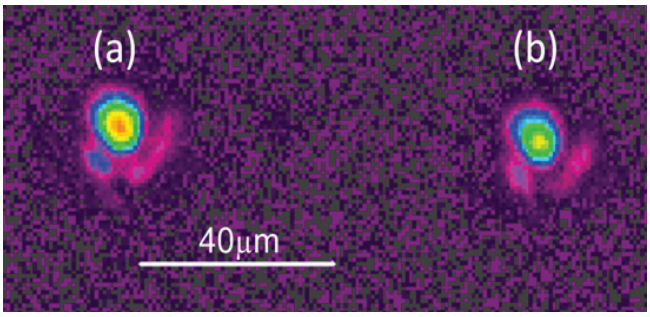

Fig. 5. Focused laser spot with (a) direct pumping and (b) DOE homogenized pumping.

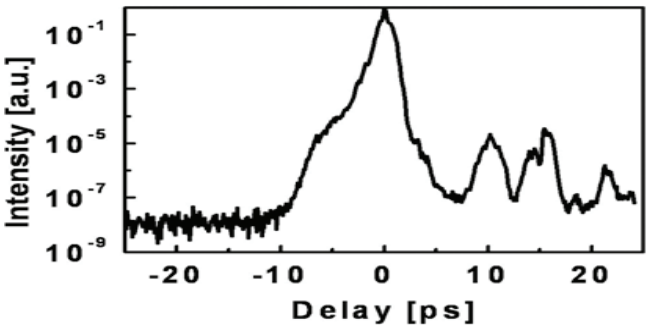

Fig. 6. Third-order autocorrelation of the amplified laser pulse pumped with a DOE homogenizer.

a third-order autocorrelator (Sequoia; Amplitude Technologies). The pulse width can be compressed to 60 fs, comparable to that with direct pumping. Figure 6 shows the third-order autocorrelation trace. The intensity ratio of the amplified spontaneous emission to the main pulse is about 10^{-8}, keeping the same as with direct pumping.

A simulation is carried out to better understand the diffraction of the amplified laser pulse. Figure 7 is the schematic diagram of the simulation. A single-mode Gaussian beam in 800-nm with a waist diameter of 8-mm propagates in the z-direction through a diffraction screen positioned at $z = 0$. The diffraction screen is divided into an array of close-packed square pupils. An intensity gain factor of M is randomly applied to each pupil. M ranges from 1 to 9, representing deposited energy density from 0 to the maximum in the speckle pattern. The pupils with $M > 1$ are noted as the amplified pupils (APs) and the remaining pupils correspond to $M = 1$. Each beamlet passing through a pupil gains a factor of M in intensity, whereas its phase keeps the same as the original. The distribution on the detection plane is the integration of all of the beamlets propagated from the diffraction screen to the detection plane, calculated with the Huygens–Fresnel principle. The dimension of the pupils approximately represents the size of the speckles in the pump beam. The aperture on the diffraction plane is circular with a diameter of 10-mm, which is the same as the crystal. The center of the aperture is on the z-axis as well as the incident beam. The detection screen is 10×10-mm.

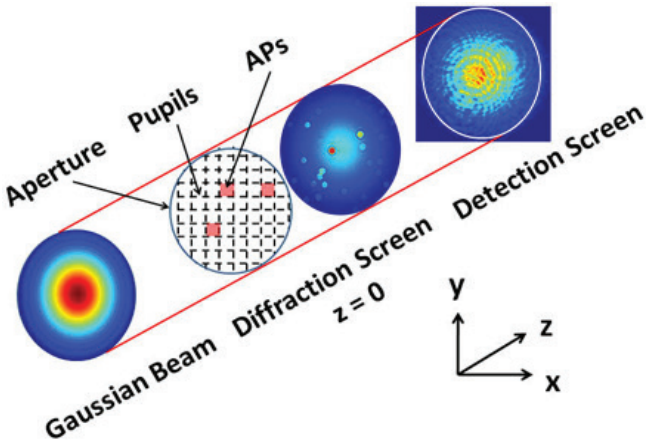

Fig. 7. The schematic diagram of the simulation.

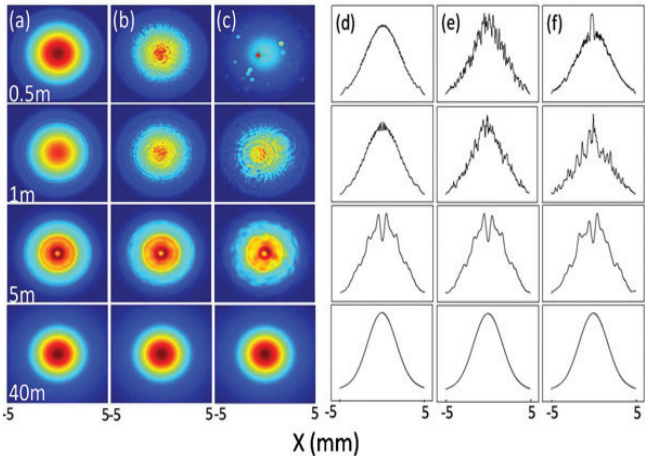

Fig. 8. Diffraction pattern and one-dimensional beam profiles on the detection screen at different distances. There is no AP in (a). The APs are with a size of 0.1×0.1 mm in (b) and 0.2×0.2 mm in (c). (d–f) One-dimensional normalized beam profiles of (a), (b), and (c), respectively.

Figure 8 shows the diffraction pattern and one-dimensional profile of Gaussian beams with AP size of 0.1×0.1-mm and 0.2×0.2-mm. As a comparison, the unamplified Gaussian beam, or a beam with no AP, is also shown in the first column. As can be seen, small "hot spots" are present only close to the diffraction plane, but quickly expand while the beam propagates further. After 5-m propagation, the two amplified beams look quite similar to the unamplified one. And after 40 m, their distributions are substantially the same as that of the unamplified beam. Due to irregular distribution of the APs, no enormous increase in intensity is obtained in the integration of the diffraction patterns. The double-peak feature in the third row is caused by the aperture diffraction and does not relate to the problem we discuss. The profile of the beam with smaller APs evolves more quickly to a smooth distribution. Therefore, smaller speckle size is preferred to get a smoother beam profile for a given propagation distance.

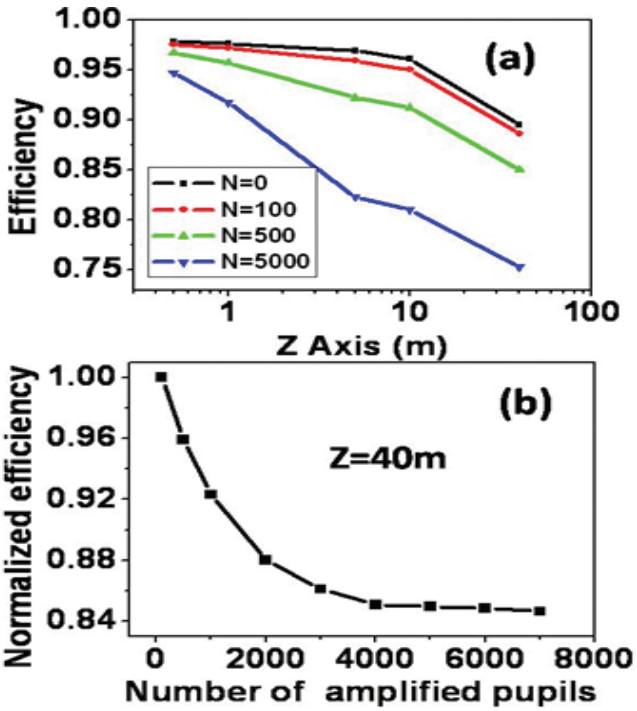

Fig. 9. (a) Propagation efficiency of beams with different number of APs and (b) beam propagation efficiency with varied APs at $z = 40$ m, normalized to that of unamplified beam.

Propagation efficiency defined as the ratio of the energy on the detection screen and the energy on the diffraction plane is studied. The dimension of the pupils used in the calculation is 0.1×0.1-mm. Figure 9(a) shows the propagation efficiencies of the unamplified Gaussian beam and three beams with a different number of APs. If we look at a single tiny amplified beamlet, it expands quickly as it propagates. However, due to coherent interference of the multiple beamlets, most part of the energy concentrates paraxially and the part far away from the axis cancels out. Increasing AP numbers results in decreased propagation efficiency. However, Fig. 9(b) indicates that the efficiency at $z = 40$ m keeps almost constant when the number of the APs are more than 4000. The minimal efficiency is about 84% of that of the unamplified Gaussian beam.

The simulation shows good agreement with the experiments in which dotted structure can be observed only in the first pass through the crystal. Double-side pumping and noncollinear overlapping of the amplified beam with the dotted pumping areas also contribute to smooth the beam. The measured high-energy propagation efficiency is also observed in the simulation, which can be as high as 84%.

In conclusion, we have tested the DOE homogenized Nd:YAG laser pumping of a multi-terawatt Ti:sapphire amplifier. Significant improvement of the amplified laser beam homogeneity is obtained, which reduces the possibility of optics damage and improves the energy extraction efficiency. The visible speckle pattern in the homogenized pump beam is not present in the final amplified beam. At the same time, no substantial negative effects are observed on the laser wavefront, the focusability, and the temporal characteristics. Hundreds of hours of operation without optical damage show that the DOEs can be safely applied to Nd:YAG laser homogenization for pumping high-power Ti:sapphire lasersystem.

This work was supported by the National Basic Research Program of China (No. 2013CBA01501) and the National Natural Science Foundation of China (Nos. 11135012 and 11375262).

References

1. M. Aoyama, K. Yamakawa, Y. Akahane, J. Ma, N. Inoue, H. Ueda, and H. Kiriyama, Opt. Lett. **28**, 1594 (2003).
2. Z. H. Wang, C. Liu, Z. W. Shen, Q. Zhang, H. Teng, and Z. Y. Wei, Opt. Lett. **36**, 3194 (2011).
3. V. Yanovsky, G. Kalinchenko, P. Rousseau, V. Chvykov, G. Mourou, and K. Krushelnick, Appl. Opt. **47**, 1968 (2008).
4. K. Ertel, C. Hooker, S. J. Hawkes, B. T. Parry, and J. L. Collier, Opt. Express **16**, 8039 (2008).
5. M. Tanaka, H. Kiriyama, Y. Ochi, Y. Nakai, H. Sasao, H. Okada, H. Daido, P. Bolton, and S. Kawanishi, Opt. Commun. **282**, 4401 (2009).
6. H. Kiriyama, M. Michiaki, Y. Nakai, T. Shimomura, H. Sasao, M. Tanaka, Y. Ochi, M. Tanoue, H. Okada, S. Kondo, S. Kanazawa, A. Sagisaka, I. Daito, D. Wakai, F. Sasao, M. Suzuki, H. Kotakai, K. Kondo, A. Sugiyama, S. Bulanov, P. R. Bolton, H. Daido, S. Kawanishi, J. L., Appl. Opt. **49**, 2105 (2010).
7. F. M. Dickey and S. C. Holswade, *Laser Beam Shaping: Theory and Techniques* (Marcel Dekker, New York, 2000).
8. S. N. Dixit, I. M. Thomas, B. W. Woods, A. J. Morgan, M. A. Henesian, P. J. Wegner, and H. T. Powell, Appl. Opt. **32**, 2543 (1993).
9. F. Canova, J. P. Chambaret, F. Reversat, S. Tisserand, F. Pie, and M. Pittman, in *CLEO'07 Conference on Lasers and Electro-Optics* 5–11 (2007).
10. P. L. E. Fabien, "Etude de l'amplification parasite transverse de la fluorescence dans les cristaux de Ti:Sa de grandes dimensions. Application à la réalisation de l'amplificateur 'petawatt' haute énergie du laser pilote de la station LASERIX", Ph.D. Thesis (L'University, Paris, 2008).
11. H. J. Teunissen, "Multipass amplifier for Terawatt Ti:sapphire laser system", Master Thesis (University of Twente, 2007).